WARSAW UNIVERSITY OF TECHNOLOGY Index 351733
FACULTY OF CIVIL ENGINEERING
COMMITTEE FOR CIVIL AND WATER ENGINEERING
POLISH ACADEMY OF SCIENCES ISSN 1230-2945
DOI: 10.24425/ace.2024.151913
ARCHIVES OF CIVIL ENGINEERING
Vol. LXX ISSUE 4 2024
pp. 615 –629

Research paper

Mechanical properties and fracture behavior of sandstone similar materials with different joint positions and thicknesses based on triaxial testing and PFC simulation

Wei Jing[1], Bingpeng Lu[2], Laiwang Jing[3], Rencai Jin[4]

Abstract: The mechanical properties and failure characteristics of joined rocks have an important impact on the disaster prevention of underground engineering and the sustainable development of mineral resources. The effects of confining pressure, joint location, and joint thickness on the mechanical properties of rock-like specimens under triaxial test have been studied. Furthermore, using the "DFN-age" function of PFC numerical simulation, the stress characteristics, and failure characteristics of rock specimens under different confining pressure, joint location and joint thickness are analyzed. The research results indicate that as the thickness of the joint increases and the joint position approaches the center of the specimen, the compressive strength of the specimen decreases. As the confining pressure increases, the compressive strength increases and failure modes of rock like specimens with different joint types also tend to be similar. The specimens manifest complex shear-tensile composite failures. In addition, the initiation cracks and main control cracks at the joint terminus can be classified as reverse tensile wing cracks, reverse shear cracks, shear cracks and tensile wing cracks. When the joint thickness of the specimen is 1.0 mm and the distance from the joint position to the center of the specimen is 10–20 mm, the crack evolution characteristics and stress distribution law of the specimen will undergo a transformation.

Keywords: different thicknesses and positions of joints, jointed rock mass, mechanical properties, spatio-temporal evolution of cracks, PFC simulation

[1]Prof., PhD., Eng., Anhui University of Science and Technology, State Key Laboratory of Mining Response and Disaster Prevention and Control in Deep Coal Mines, 168 Taifeng Street, Huainan City, Anhui Province, China, e-mail: wjing@aust.edu.cn, ORCID: 0000-0002-0256-7655

[2]M.Sc., Anhui University of Science and Technology, School of Civil Engineering and Architecture, 168 Taifeng Street, Huainan City, Anhui Province, China, e-mail: 2420620107@qq.com, ORCID: 0009-0001-4468-0349

[3]Prof., PhD., Eng., Anhui University of Science and Technology, State Key Laboratory of Mining Response and Disaster Prevention and Control in Deep Coal Mines, 168 Taifeng Street, Huainan City, Anhui Province, China, e-mail: lwjing229@126.com, ORCID: 0000-0003-3131-8786

[4]Eng., China MCC17 Group Co., LTD., Civil Engineering Post-doctoral Research Workstation, No. 88 Yushan East Road, Huashan District, Ma'anshan City, Anhui Province, China, e-mail: zgsqy17@sina.com, ORCID: 0000-0002-8028-3658

1. Introduction

Jointed rocks in large-scale rock projects like mines, tunnels, and water conservancy can significantly affect the stability of underground rock, impacting project construction and mineral mining. The diverse types, sizes, and distribution of joints complicate the mechanical properties and failure of rocks [1–3]. Therefore, studying the mechanical characteristics and joint evolution dynamics of fractured rock masses under load is crucial for ensuring safety and stability in rock engineering projects.

The current research approaches for studying fractured rock masses encompass real rock material testing, model material testing, and numerical simulation methods. Some scholars [4–7] create standard rock specimens from natural rock masses and use cutting equipment to simulate natural fractured rocks for research purposes. For instance, Yang [8] and Tian et al. [9] explored fracture evolution characteristics of double-jointed rock through uniaxial compression tests and PFC numerical simulation. Morgan et al. [10] analyzed the deformation and failure tendencies of granite specimens with joints of different angles using uniaxial compression tests. Moreover, extensive research has been conducted on rock-like specimens in recent years, supporting the scientific validity of using such materials to emulate natural rocks [11–14]. Jin et al. [15] studied the energy mechanism and failure characteristics of single joint rock specimens under uniaxial compression at different angles. Selçuk et al. [16] conducted experimental studies on the strength and failure behavior evolution mechanism of rock concrete bimaterial interface under different angles using various testing methods. Asadizadeh et al. [17] elucidated the influence of differing joint roughness, bridge lengths, bridge angles, and joint angles on the mechanical behavior and joint development within rock-like specimens subjected to uniaxial compression.

In relevant research, the influence of joint thickness and joint location on the mechanical properties and failure characteristics of rock masses has received scant attention. This investigation has unveiled the mechanical properties and crack propagation behavior of rock-like specimens distinguished by differing confining pressures, joint locations, and joint thicknesses under triaxial compression. This study can provide a reference for the stability control of joined rock mass in deep underground engineering.

2. Experimental study

2.1. Preparation of test specimens

The experimental results show that cement mortar is an ideal similar material for rock model, which can efficiently simulate the properties of natural rock [18–21]. In this paper, the river sand with good gradation is selected as aggregate, and the particle size is not larger than 1.25 mm. The binder is clay and P.O 42.5 ordinary Portland cement.

The specification used for this test mold is 150 ×150 ×300 mm, joints conforming to various predetermined types are cut on both surfaces of a 150 ×150 mm test mold. Subsequently, steel sheets corresponding to the required joint patterns are inserted to produce the joint test die

essential for this study. The mold is shown in Fig. 1, and the distribution location of joints in the mold is shown in Fig. 2. The variable *h*represents the vertical distance from the joint location to the center of the test piece, while *d* represents the thickness of the respective joint.

Fig. 1. Test mold and rock-like specimens with joints

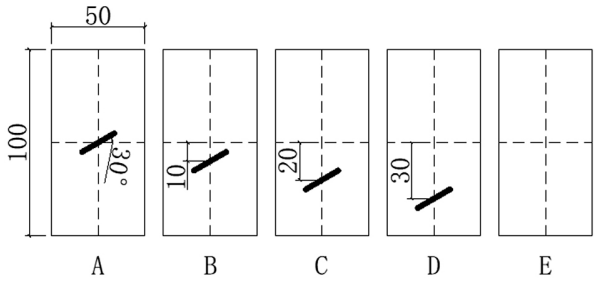

Fig. 2. Joint types of rock-like specimens in test

According to the thickness of natural rock joints, these joints can be categorized as wide tensile joints (d >5 mm), open joints (3 mm ≤ d ≤ 5 mm), micro tensile joints (1 mm ≤ d ≤ 3 mm), and closed joints (d <1 mm). This study primarily focuses on common closed joints and micro tensile joints, with selected joint thicknesses of 0.3 mm, 0.6 mm, 1.0 mm, and 1.5 mm, and distribution positions of 0 mm, 10 mm, 20 mm, and 30 mm, respectively. For the control group, complete specimens without joints are employed. The joints in this test are all through joints with a width l of 20 mm and an angle α of 30 degrees.

The manufacturing process of the rock-like specimens in this study involves a composition ratio of cement, river sand, clay, and water at 1.0:1.7:0.1:0.45. To reduce internal porosity and achieve a closer approximation to real rock, a defoaming agent comprising 0.06% of the total cement mortar mass is included. The specific test conditions are outlined in Table 1, where h denotes the distance from joint location to the specimen center, and d represents joint thickness in the specimens.

Table 1. Test conditions of rock-like specimens with different thickness and distribution of joints

No.	*h* [mm]	*d* [mm]	No.	*h* [mm]	*d* [mm]
A1	0	0.3	C1	20	0.3
A2	0	0.6	C2	20	0.6
A3	0	1.0	C3	20	1.0
A4	0	1.5	C4	20	1.5
B1	10	0.3	D1	30	0.3
B2	10	0.6	D2	30	0.6
B3	10	1.0	D3	30	1.0
B4	10	1.5	D4	30	1.5
			E	–	–

2.2. Test scheme and equipment

The uniaxial compression test and triaxial compression test in this paper were completed by MTS-816 electro-hydraulic servo triaxial testing machine of State key Laboratory of Mining response and disaster Prevention and Control in Deep Coal Mines of Anhui University of Science and Technology, as shown in Fig. 3. Confining pressure values were set at 0 MPa, 4 MPa, and 8 MPa, with the loading rate maintained at 100 N/s. To guarantee the accuracy of the test data, at least three tests were conducted for each group of fractured rock specimens.

Fig. 3. MTS-816 electro-hydraulic servo triaxial testing machine

3. Analysis of experimental results

Figure 4 present the variation curves illustrating the alterations in compressive strength for rock-like specimens, contingent upon various joint thicknesses and distribution positions, while subjected to three distinct confining pressures. Evidently, these figures elucidate that

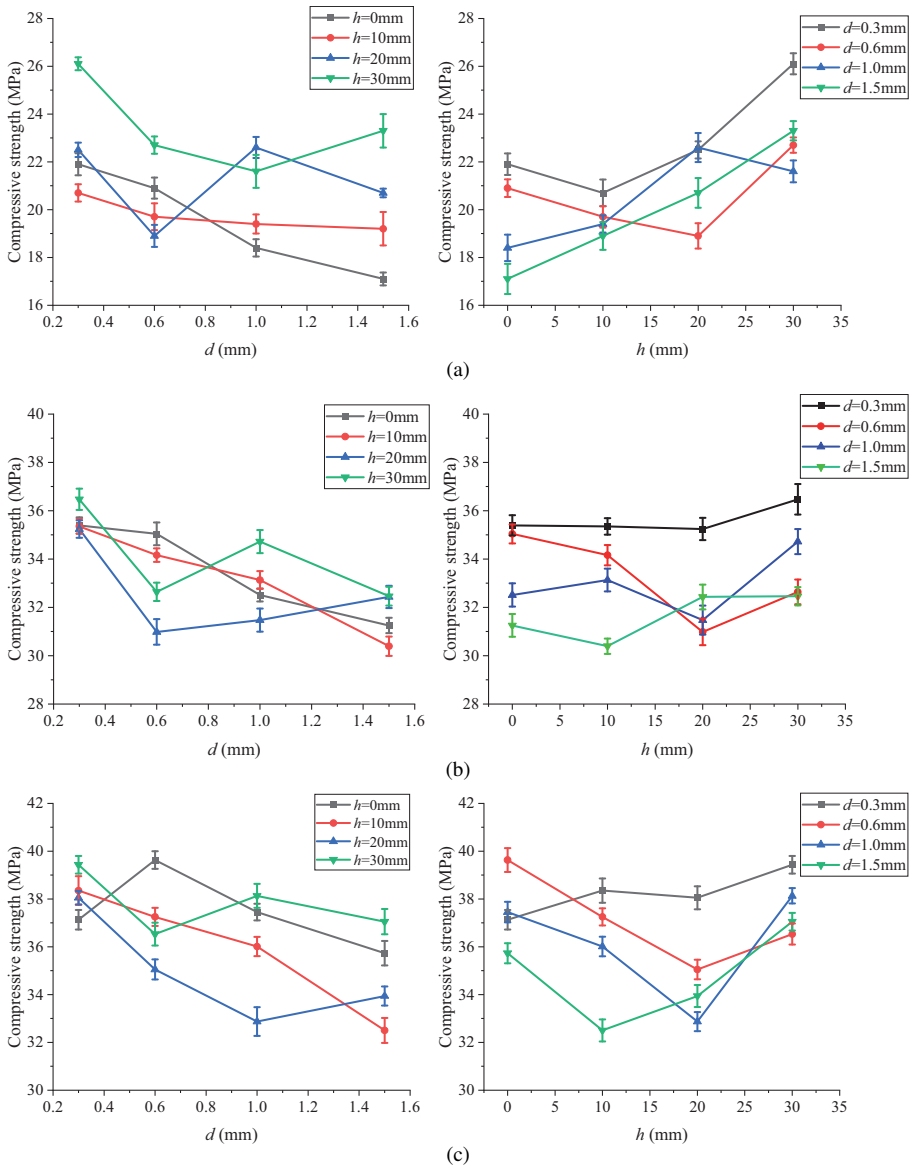

Fig. 4. Influence of joint location and thickness on compressive strength of rock-like specimens under different confining pressure: (a) 0 MPa, (b) 4 MPa, (c) 8 MPa

the compressive strength of specimens featuring joints has experienced a significantly decline in comparison to their intact counterparts, and its compressive strength is about 45% of the uniaxial compressive strength of complete rock specimens. It can be seen that through joints have a relatively significant weakening effect on rock strength.

3.1. Effect of joint thickness on compressive strength of specimen

Under consistent confining pressure conditions, it is discernible that the compressive strength of specimens at each joint distribution location diminishes with escalating joint thickness. However, as the joint distribution location approaches the end of the specimens, a distinctive shift occurs: the compressive strength of the test specimen transitions from a continuous decrement to an initial decrease followed by a subtle increment as the joint thickness increases. The critical joint location for this regular change is $h = 20$ mm. Furthermore, when the confining pressure remains constant, the extent of attenuation in compressive strength for specimens positioned at varying joint distribution locations diminishes progressively with an augmented distance from the joint distribution location to the specimen's center. It becomes evident that, as joint thickness increases, the susceptibility of compressive strength to joint thickness experiences a gradual reduction.

3.2. Effect of joint position on compressive strength of specimen

As the joint thickness remains constant, the compressive strength of the specimen generally increases as the joint location approaches the end. Additionally, as the confining pressure increases, the rate of growth in compressive strength gradually diminishes and tends to stabilize. Consequently, an increase in confining pressure leads to a gradual reduction in the joint's impact on the compressive strength of the specimens. Furthermore, under various confining pressures, the slope of each curve increases as the joint location continues to approach the end. It becomes evident that the sensitivity of compressive strength to joint location intensifies as the joint's position nears the specimen's terminus.

4. Numerical simulation based on PFC

The type and location of joints in rock masses exert a direct impact on internal stress distribution, which subsequently affects the mechanical properties and crack evolution characteristics of rock mass. In order to study the spatio-temporal evolution mechanism of crack growth of rock-like specimens with different cracks, the fracture characteristics of specimens was revealed based on the "DFN age" function of PFC numerical simulation software. Finally, the effects of joint location and thickness on the stress and path of crack growth and failure mode of rock-like specimens can be analyzed.

Referring to the study of Yang [8], the types of cracks are shown in Fig. 5. A two-dimensional parallel bond model is established by using PFC 2D particle flow software. The size of the model is 50 mm (wide) ×100 mm (high), which can transmit the characteristics of force and torque at the same time, and reflects the mechanical properties of rock-like specimens. The mechanical properties and failure modes of rock-like specimens with joints can be simulated and analyzed by using PFD model [22–24].

During the simulation, the "trial and error method" was used to adjust the parameters, so that the mechanical properties and failure form of the specimen obtained were similar to the

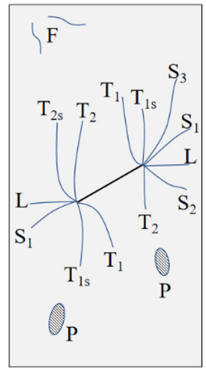

Fig. 5. Cracks types in jointed rock-like specimens: T_1 – tensile wing crack, T_{1S} – secondary tensile crack, T_{2S} – anti-tensile wing crack, T_{2S} – secondary tensile crack, S_2 – anti-shear crack, S_3 – secondary shear crack, S_1 – primary shear crack, L – transverse crack, P – surface exfoliation, F – far field crack

experimental results. The difference between the elastic modulus, Poisson's ratio, and ultimate compressive strength (UCS) of the PFC model and the rock like experimental specimens shall not exceed 2%. Other microscopic mechanical parameters in PFC numerical simulation are shown in Table 2.

Table 2. Microscopic mechanical paramenters of PFC model

Parameters	Value	Parameters	Value
Maximum particle diameter (mm)	0.20	Deformation modulus of parallel bond (GPa)	8.32
Minimum particle diameter (mm)	0.15	Stiffness ratio of parallel bond	1.89
Density (kg/m^3)	2000	Cohesion of parallel bone (MPa)	8.45
Friction coefficient	0.5	Tensile strength of parallel bond (MPa)	2
Contact modulus of particle (GPa)	1	Friction angle of parallel bond (°)	15
Porosity	0.1	Friction cofficient of parallel bond	0.25

4.1. Effect of joint thickness and position on fracture characteristics of rock-like specimens

The "DFN age" function of PFC particle flow numerical simulation software has been innovatively utilized for modeling and analysis, and the fracture characteristics of rock-like specimens have been analyzed by clearly marking crack positions at different times with different colors, as shown in Fig. 6–8.

Due to the fact that when the joint thickness is small, the crack evolution law does not change much, rock-like specimens with joint thicknesses of 0.6 mm, 1.0 mm, and 1.5 mm were selected for numerical modeling and analysis. Throughout the process, cracks generated

at different times were represented in diverse colors. Throughout the entire process, the time when the red cracks occur corresponds to the start of the specimen cracking, while the time when the blue cracks occur corresponds to the final failure of the specimen.

4.1.1. Fracture characteristics of rock-like specimens with joints of different thickness and position under uniaxial compression

Figure 6 depicts the analysis diagram of crack evolution behavior and failure pattern of rock-like specimens under uniaxial compression. The prevailing failure mode is one of shear-tensile composite failure.

It can be seen from Fig. 6 that when the joint thickness measures 0.6 mm, regardless of the location of the crack in the specimen, the types of initiation cracks at the joint tip are basically the same, all of which are anti tensile wing cracks and anti shear cracks. When the

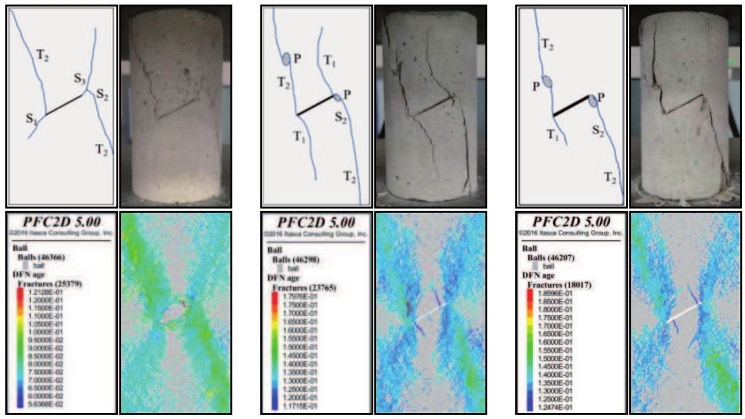

(a)

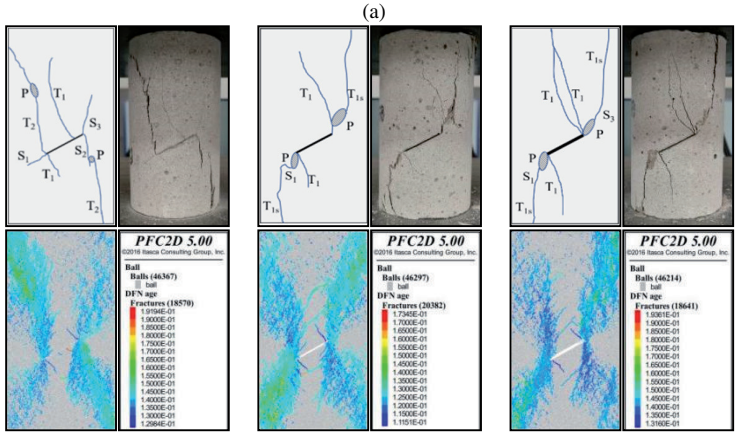

(b)

Fig. 6. The failure modes and crack evolution behavior of specimens under uniaxial compression conditions: (a) A2, A3, A4, (b) B2, B3, B4, (c) C2, C3, C4, (d) D2, D3, D4

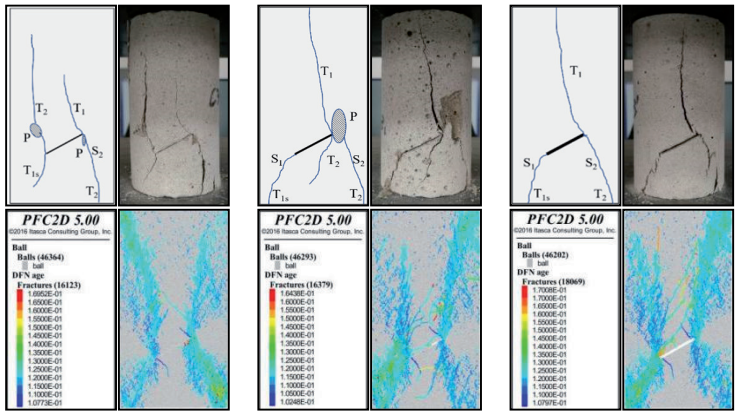

(c)

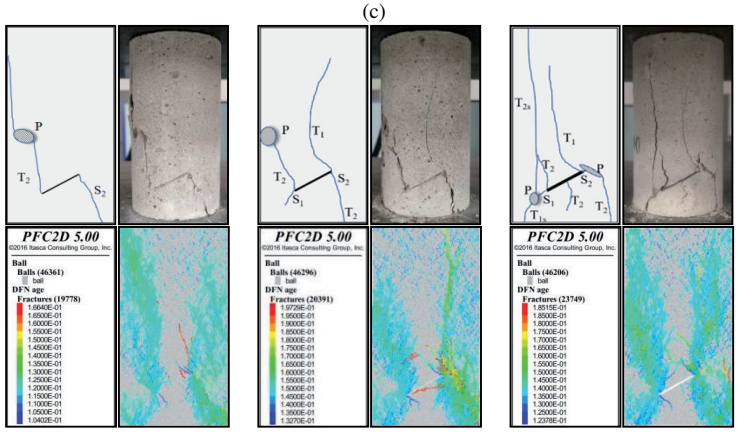

(d)

Fig. 6. [cont]

joint thickness of the specimen is greater than or equal to 1.0 mm, the type of initiation cracks at the joint tips also changes continuously as the joint position changes from the center of the specimen. Furthermore, under uniaxial compression conditions, the crack evolution behavior and failure mode of specimens featuring joint thicknesses of 1.0 mm and 1.5 mm are relatively similar at each joint location.

4.1.2. Fracture characteristics of rock-like specimens with joints of different thickness and position under confining pressure of 4 MPa

Figure 7 illustrates the failure types and joint development characteristics of specimens under varying joint positions and thickness conditions, as ascertained through numerical simulations at a confining pressure of 4 MPa. As the position of joints moves from the center of the specimen to the lower part of the specimen end, the development of joints becomes more complex, with a large number of secondary cracks concentrated at the lower end of

the specimen, and a significant increase in the number of fine cracks generated around the joints. These secondary cracks proliferate and coalesce into the primary controlling cracks, culminating in specimen failure dominated by the primary controlling cracks. The prevailing failure mode is one characterized by a complex shear-tensile composite failure.

It can be seen that when the confining pressure is 4 MPa, the development types of joints are basically consistent with the changes in the location of joints when the joint thickness is 0.6 mm and 1.0 mm. For these two thickness categories, For these two types of joint thicknesses, there is no significant change in the type of cracks in the specimen when the joint location is no more than 10 mm from the center of the specimen. When the position of joints exceeds 10 mm from the center of the specimen, the joints type in the specimen suddenly changes. When the joint is located at the center of the specimen and 30 mm away from the center of the specimen, the cracks development characteristics of the specimens with joint thickness of 1.5 mm are

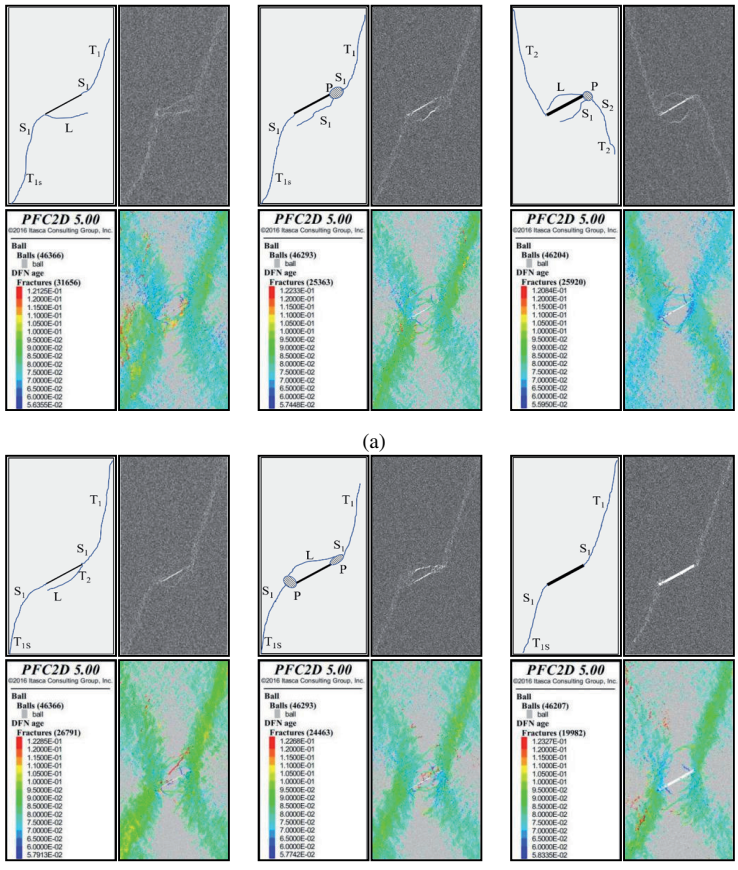

Fig. 7. The failure types and crack evolution behavior of specimens under confining pressure of 4 MPa: (a) A2, A3, A4, (b) B2, B3, B4, (c) C2, C3, C4, (d) D2, D3, D4

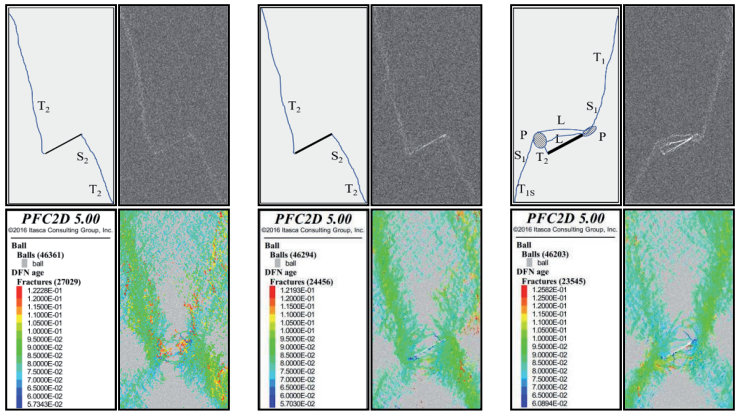

(c)

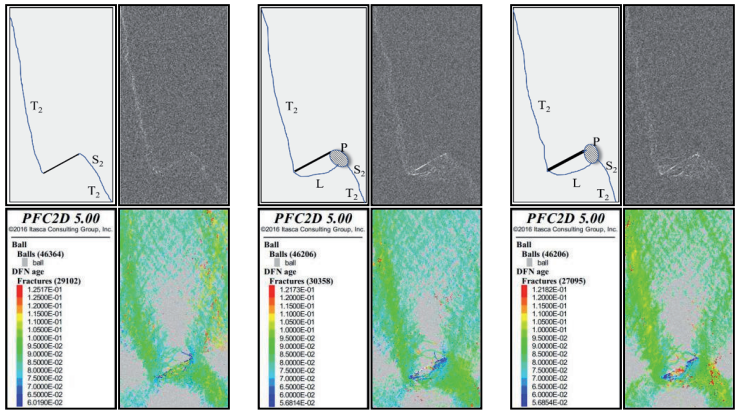

(d)

Fig. 7. [cont]

obviously different from those of other thicknesses. When the position of the joint is 10 mm and 20 mm from the center of the specimen, the change of the joint thickness has no obvious effect on the cracks development characteristics.

4.1.3. Fracture characteristics of rock-like specimens with joints of different thickness and position under confining pressure of 8 MPa

Figure 8 illustrates failure types and crack evolution behavior of specimens subjected to an 8 MPa confining pressure. When the joint is centrally situated within the specimen, its primary governing cracks transition from anti-shear cracks to tensile-type cracks over the course of development, gradually penetrating towards the extremities of the specimens culminating in failure. This fracture mode manifests as a shear-tensile composite failure.

Therefore, when the confining pressure is 8 MPa, the types of initiation cracks and later development cracks in group A are both anti-tensile wing shaped cracks and anti-shear cracks.

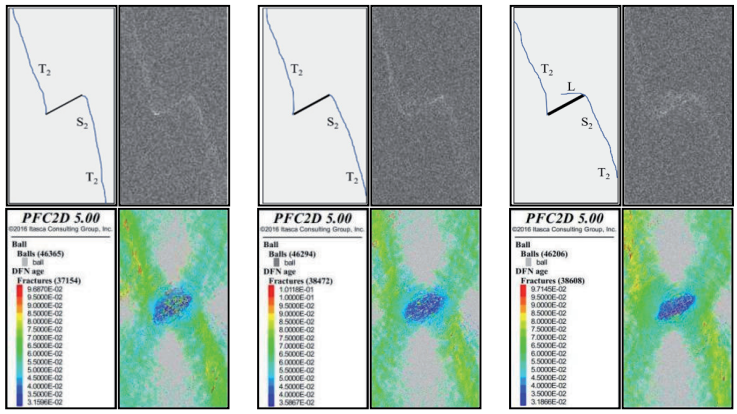

(a)

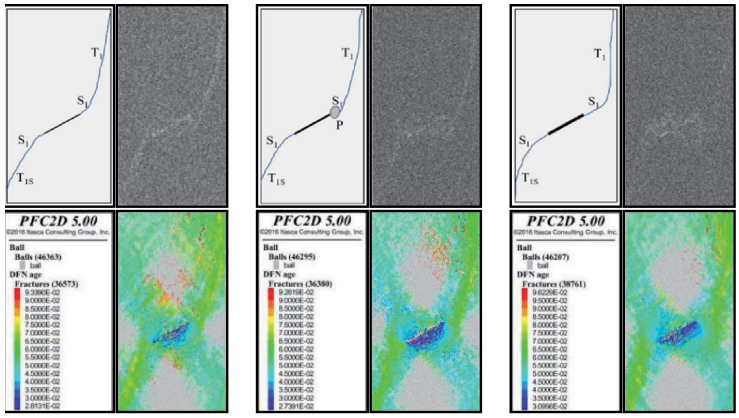

(b)

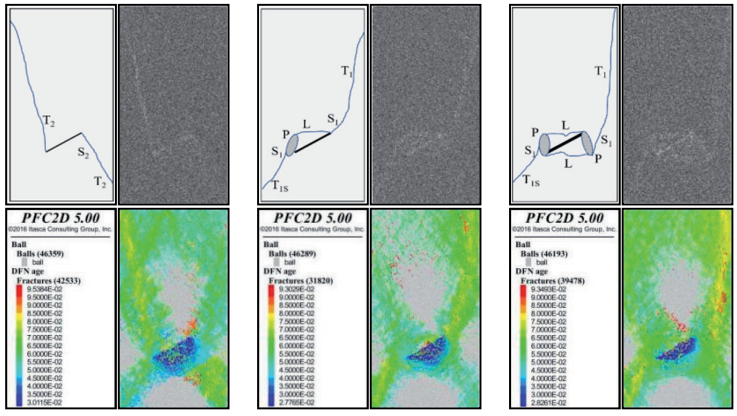

(c)

Fig. 8. The failure types and crack evolution behavior of specimens under confining pressure of 8 MPa: (a) A2, A3, A4, (b) B2, B3, B4, (c) C2, C3, C4, (d) D2, D3, D4

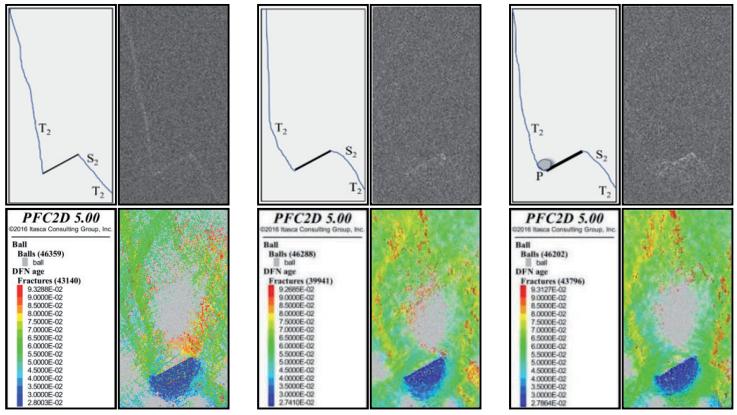

(d)

Fig. 8. [cont]

The types of initiation cracks and later developed cracks in group B are basically shear cracks and tensile wing cracks. The types of initial cracks and later developed cracks in group C are mainly shear cracks and tensile wing cracks, accompanied by a small amount of anti-tensile wing cracks. The types of initiation cracks and later development cracks in group D are mainly shear cracks, tensile wing cracks, and anti-tensile wing cracks. With this confining pressure, except for the joint located 20 mm from the specimen's center and possessing a 1.0 mm thickness, the failure evolution behavior of rock specimens with different joint thicknesses at the same joint location is basically similar to the joint type, which means that the change in joint thickness has little impact on the joints development characteristics. The ultimate failure type is shear tensile composite failure.

In summary, based on mechanical tests and PFC numerical simulation results, it can be concluded that rock like specimens with joints of different thicknesses and positions will undergo complex shear tensile composite failure. There are two main types of joint tip initiation cracks and main control cracks: anti tensile wing cracks and anti shear cracks, or shear cracks and tensile wing cracks. Taking the case when the joint thickness is 1.0 mm and the joint position is 10 mm to 20 mm away from the center of the specimen as the turning point, the crack propagation and evolution law of the specimen will undergo significant changes.

5. Conclusions

This article systematically examines the mechanical properties and crack propagation behavior of rock-like specimens under various joint thicknesses and positions. The findings can offer valuable insights for the stability control of surrounding rock in underground engineering and the sustainable development of mineral resources. Based on the studies, the following conclusions can be drawn:

1. The mechanical properties of jointed rock-like specimens under different confining pressure, joint position, and joint thickness were analyzed using triaxial compression

tests. As the thickness of the joint increases and the joint position approach the center of the specimen, the compressive strength of the specimen decreases. When the confining pressure increases, the compressive strength increases. The influence of joint location and thickness on the compressive strength of the specimen continues to decrease. The initiation stress characteristics, failure modes, and fracture types of rock like specimens with different joint types also tend to be similar.

2. The fracture mode of rock-like specimens with different thickness and position joints is a complex shear-tensile composite failure. There are two main types of joint tip initiation cracks and main control cracks: anti-tensile wing cracks and anti-shear cracks, or shear cracks and tensile wing cracks.
3. When the joint thickness of the specimen is 1.0 mm and the distance between the joint position and the center of the specimen is 10–20 mm, the fracture mode and stress distribution of the specimen will change fundamentally. Therefore, the essential change of the type of joint and the law of stress distribution will have an important influence on the mechanical properties and crack propagation law of rock mass in practical engineering.

Acknowledgements

This study was supported by the Major Project Of Natural Science Research Project of Anhui Educational Committee (KJ2021ZD0053), the National Natural Science Foundation of China (51904012), the Open Fund of State Key Laboratory of Mining Response and Disaster Prevention and Control in Deep Coal Mine (SKLMRDPC19KF02), the Project Supported By Scientific Research Activities Of Postdoctoral Researchers In Anhui Province (2022B640).

References

[1] C. Caselle, S. Bonetto, C. Comina, and S. Stocco, "GPR surveys for the prevention of karst risk in underground gypsum quarries", *Tunnelling and Underground Space Technology*, vol. 95, art. no. 103137, 2020, doi: 10.1016/j.tust.2019.103137.

[2] S. Zhang, Y. Li, H. Liu, and X. Ma, "Experimental investigation of crack growth behavior and failure characteristics of cement infilled rock", *Construction and Building Materials*, vol. 268, art. no. 121735, 2021, doi: 10.1016/j.conbuildmat.2020.121735.

[3] S. Hao, R. Fei, and J. Yu, "Mechanical characteristics of ultra-shallow buried high-speed railway tunnel in broken surrounding rock during construction", *Archives of Civil Engineering*, vol. 68, no. 3, pp. 645–659, 2022, doi: 10.24425/ace.2022.141908.

[4] R.H. Cao, R. Yao, H. Lin, Q.B. Lin, Q. Meng, and T. Li, "Shear behaviour of 3D nonpersistent jointed rock-like specimens: Experiment and numerical simulation", *Computers and Geotechnics*, vol. 148, art. no. 104858, 2022, doi: 10.1016/j.compgeo.2022.104858.

[5] L.X. Xiong, H. Chen, X. Gao, Z. Xu, and D. Hu, "Experimental study on biaxial dynamical compressive test and PFC2D numerical simulation of artificial rock sample with single joint", *Archives of Civil Engineering*, vol. 69, no. 1, pp. 213–229, 2023, doi: 10.24425/ace.2023.144169.

[6] Z. Aliabadian, G.F. Zhao, and A.R. Russell, "Crack development in transversely isotropic sandstone discs subjected to Brazilian tests observed using digital image correlation", *International Journal of Rock Mechanics and Mining Sciences*, vol. 119, pp. 211–221, 2019, doi: 10.1016/j.ijrmms.2019.04.004.

[7] S. Bastola and M. Cai, "Investigation of mechanical properties and crack growth in pre-cracked marbles using lattice-spring-based synthetic rock mass (LS-SRM) modeling approach", *Computers and Geotechnics*, vol. 110, pp. 28–43, 2019, doi: 10.1016/j.compgeo.2019.02.009.

[8] S.Q. Yang, "Crack coalescence behavior of brittle sandstone samples containing two coplanar joints in the process of deformation failure", *Engineering Fracture Mechanics*, vol. 78, no. 17, pp. 3059–3081, 2011, doi: 10.1016/j.engfracmech.2011.09.002.

[9] W. L. Tian, S. Q. Yang, and Y. H. Huang, "PFC2D simulation on crack evolution behavior of brittle sandstone containing two coplanar joints under different confining pressures", *Journal of Mining and Safety Engineering*, vol. 34, no. 6, pp. 1207, 2017, doi: 10.13545/j.cnki.jmse.2017.06.026.

[10] S.P. Morgan, C.A. Johnson, and H.H. Einstein, "Cracking processes in Barre granite: fracture process zones and crack coalescence", *International Journal of Fracture*, vol. 180, no. 2, pp. 177–204, 2013, doi: 10.1007/s10704-013-9810-y.

[11] L.X. Xiong, H. Chen, Z. Xu, and D. Hu, "Uniaxial compression test and numerical simulation of rock-like specimen with T-Shaped cracks", *Archives of Civil Engineering*, vol. 69, no. 2, pp. 227–244, 2023, doi: 10.24425/ace.2023.145265.

[12] X. Li, W. Gao, L. Guo, Z. Li, and S. Zhang, "Influences of the number of non-consecutive joints on the dynamic mechanical properties and failure characteristics of a rock-like material", *Engineering Failure Analysis*, vol. 146, art. no. 107101, 2023, doi: 10.1016/j.engfailanal.2023.107101.

[13] Z. Wang, J. Zhou, and L. Li, "Fracture mechanical properties of rock-like materials under half symmetric loading", *Archives of Civil Engineering*, vol. 63, no. 4, pp. 71–82, 2017, doi: 10.1515/ace-2017-0041.

[14] Y. Liu, F. Dai, T. Zhao, and N.W. Xu, "Numerical investigation of the dynamic properties of intermittent jointed rock models subjected to cyclic uniaxial compression", *Rock Mechanics and Rock Engineering*, vol. 50, pp. 89–112, 2017, doi: 10.1007/s00603-016-1085-y.

[15] J. Jin, P. Cao, Y. Chen, C. Pu, D. Mao, and X. Fan, "Influence of single flaw on the failure process and energy mechanics of rock-like material", *Computers and Geotechnics*, vol. 86, pp. 150–162, 2017, doi: 10.1016/j.compgeo.2017.01.011.

[16] L. Selçuk and D. Aşma, "Experimental investigation of the rock-concrete bi materials influence of inclined interface on strength and failure behavior", *International Journal of Rock Mechanics and Mining Sciences*, vol. 123, art. no. 104119, 2019, doi: 10.1016/j.ijrmms.2019.104119.

[17] M. Asadizadeh, M.F. Hossaini, M. Moosavi, H. Masoumi, and P.G. Ranjith, "Mechanical characterisation of jointed rock-like material with non-persistent rough joints subjected to uniaxial compression", *Engineering Geology*, vol. 260, art. no. 105224, 2019, doi: 10.1016/j.enggeo.2019.105224.

[18] M. Sharafisafa, Z. Aliabadian, F. Tahmasebinia, and L. Shen, "A comparative study on the crack development in rock-like specimens containing unfilled and filled flaws", *Engineering Fracture Mechanics*, vol. 241, art. no. 107405, 2021, doi: 10.1016/j.engfracmech.2020.107405.

[19] Z. Zhao, H. Jing, X. Shi, and G. Han, "Experimental and numerical study on mechanical and fracture behavior of rock-like specimens containing pre-existing holes flaws", *European Journal of Environmental and Civil Engineering*, vol. 26, no. 1, pp. 299–319, 2022, doi: 10.1080/19648189.2019.1657961.

[20] M. Teng, J. Bi, Y. Zhao, and C. Wang, "Experimental study on shear failure modes and acoustic emission characteristics of rock-like materials containing embedded 3D flaw", *Theoretical and Applied Fracture Mechanics*, vol. 124, art. no. 103750, 2023, doi: 10.1016/j.tafmec.2023.103750.

[21] S. Zhou, X. Zhuang, and T. Rabczuk, "Phase field modeling of brittle compressive-shear cracks in rock-like materials: A new driving force and a hybrid formulation", *Computer Methods in Applied Mechanics and Engineering*, vol. 355, pp. 729–752, 2019, doi: 10.1016/j.cma.2019.06.021.

[22] Y. Chen, H. Lin, S. Xie, X. Ding, D. He, W. Yong, and F. Gao, "Effect of joint microcharacteristics on macroshear behavior of single-bolted rock joints by the numerical modelling with PFC", *Environmental Earth Sciences*, vol. 81, no. 10, art. no. 276, 2022, doi: 10.1007/s12665-022-10411-y.

[23] J. Ren, M. Xiao, and G. Liu, "Rock Macro-Meso Parameter Calibration and Optimization Based on Improved BP Algorithm and Response Surface Method in PFC 3D", *Energies*, vol. 15, no. 17, art. no. 6290, 2022, doi: 10.3390/en15176290.

[24] W.Y. Li, C. Shi, and C. Zhang, "Numerical study on the effect of grain size on rock dynamic tensile properties using PFC-GBM", *Computational Particle Mechanics*, vol. 11, pp. 481–489, 2024, doi: 10.1007/s40571-023-00634-6.

Received: 2023-12-21, Revised: 2024-04-16